

# Low Rate Sampling of Pulse Streams with Application to Ultrasound Imaging

Ronen Tur, Yonina C. Eldar, *Senior Member, IEEE* and Zvi Friedman

**Abstract**—Signals comprised of a stream of short pulses appear in many applications including bio-imaging, radar, and ultrawideband communication. Recently, a new framework, referred to as finite rate of innovation, has paved the way to low rate sampling of such pulses by exploiting the fact that only a small number of parameters per unit time are needed to fully describe these signals. Unfortunately, for high rates of innovation, existing approaches are numerically unstable. In this paper we propose a general sampling approach which leads to stable recovery even in the presence of many pulses. We begin by deriving a condition on the sampling kernel which allows perfect reconstruction of periodic streams of pulses from a minimal number of samples. This extends previous work which assumes that the sampling kernel is an ideal low-pass filter. A compactly supported class of filters, satisfying the mathematical condition, is then introduced, leading to a sampling framework based on compactly supported kernels. We then extend our periodic solution to finite and infinite streams, and show that our method is numerically stable even for a large number of pulses per unit time. High noise robustness is demonstrated as well when the time delays are sufficiently separated. Finally, we apply our results to ultrasound imaging data, and show that our techniques result in substantial rate reduction with respect to traditional ultrasound sampling schemes.

**Index Terms**—Analog-to-digital conversion, annihilating filters, finite rate of innovation, generalized sampling, perfect reconstruction, ultrasound imaging.

## I. INTRODUCTION

**S**AMPLING is the process of representing a continuous-time signal by discrete-time coefficients, while retaining the important features present in the analog signal. The well-known Shannon-Nyquist theorem states that the minimal sampling rate required for perfect reconstruction of bandlimited signals is twice the maximal frequency, and describes a sampling and reconstruction scheme which achieves this minimal rate. This result has been generalized to minimal rate sampling schemes for signals lying in an arbitrary subspace [1], [2].

Recently, there has been growing interest in sampling of signals consisting of a stream of short pulses, where the pulse shape is known. Such signals have a finite number of degrees of freedom per unit time, also known as the Finite Rate of Innovation (FRI) property [3]. This interest is motivated by applications such as digital processing of neuronal signals, bio-imaging, image processing and ultrawideband (UWB) communications, where such signals are present in abundance. Our work is motivated by the possible application of this

model in ultrasound imaging. Ultrasound images are formed by transmitting an ultrasonic pulse into a tissue. Echoes of the pulse bounce off scatterers within the tissue, and create a signal consisting of a stream of pulses at the receiver. The time-delays and amplitudes of the echoes indicate the position and strength of the various scatterers, respectively. Therefore, determining these parameters from low rate samples of the received signal is an important problem. Reducing the rate allows more efficient processing which can translate to power and size reduction of the ultrasound imaging system.

Our goal is to design a minimal rate single-channel sampling and reconstruction scheme for pulse streams that is stable even in the presence of many pulses. Since the set of FRI signals does not form a subspace, classic subspace schemes cannot be directly used to design low-rate sampling schemes. Mathematically, FRI signals conform with a broader model of signals lying in a union of subspaces [4]–[8]. Although the minimal sampling rate required for such settings has been derived, no generic sampling scheme exists for the general problem. Nonetheless, some special cases have been treated in previous work, including streams of pulses.

A stream of pulses can be viewed as a parametric signal, uniquely defined by the time-delays of the pulses and their amplitudes. An efficient sampling scheme for periodic streams of impulses, having  $L$  impulses in each period, was proposed in [3], [9]. This sampling scheme allows to obtain a set of Fourier series coefficients of the periodic signal. Once these coefficients are known, the problem of determining the time-delays and amplitudes of the pulses becomes that of finding the frequencies and amplitudes of a sum of sinusoids. The latter is a standard problem in spectral analysis [10] which can be solved using conventional methods, such as the annihilating filter approach, as long as the number of samples is greater than  $2L$ . This result is intuitive since  $2L$  is the number of degrees of freedom in each period:  $L$  time-delays and  $L$  amplitudes.

Periodic streams of pulses are mathematically convenient to analyze, however not very practical. In contrast, finite streams of pulses are prevalent in applications such as ultrasound imaging. The first treatment of finite Dirac streams appears in [3], in which a Gaussian sampling kernel was proposed. The time-delays and amplitudes are then estimated from the Gaussian tails. This method and its improvement [11] are numerically unstable for high rates of innovation, since they rely on the tails of the Gaussians which take on low values. A different approach based on moments of the signal was developed in [12], where the sampling kernels have compact time support. This method treats streams of Diracs, differentiated Diracs, and short pulses with compact support and no DC

Department of Electrical Engineering, Technion—Israel Institute of Technology, Haifa 32000, Israel. Phone: +972-4-8293256, fax: +972-4-8295757, E-mail: {ronentur@technix, yonina@ee}.technion.ac.il, zvi.friedman@med.ge.com. This work was supported in part by a Magnetron grant from the Israel Ministry of Industry and Trade.

component. However, the authors point out that this sampling scheme is numerically unstable for large  $L$ . To the best of our knowledge, a numerically stable sampling and reconstruction scheme (when the delays are sufficiently separated) for high order problems has not yet been reported.

Infinite streams of pulses arise in applications such as UWB communications, where the communicated data changes frequently. Using a compactly supported filter [12], and under certain limitations on the signal, the infinite stream can be divided into a sequence of separate finite problems. The individual finite cases may be treated using methods for the finite setting, however this leads to a sampling rate that is higher than the rate of innovation. Since the infinite stream reconstruction scheme is based on the finite one, the instability in high order problems applies here as well. In addition, the constraints that are cast on the signal become more and more stringent as the number of pulses per unit time grows. In a recent work [13] the authors propose a sampling and reconstruction scheme for finite and infinite streams of dirac impulses for the restricted case in which there is no more than one impulse per sampling period. This may be viewed as a reduction of the infinite setting to a sequence of finite stream problems, each with  $L = 1$ . Our interest here is in high values of  $L$ .

Another related work [7] proposes a semi-periodic model, where the pulse time-delays do not change from period to period, but the amplitudes vary. This is a hybrid case in which the number of degrees of freedom in the time-delays is finite, but there is an infinite number of degrees of freedom in the amplitudes. Therefore, the proposed recovery scheme generally requires an infinite number of samples. This differs from the periodic and finite cases we discuss in this paper which have a finite number of degrees of freedom and, consequently, require only a finite number of samples.

In this paper we study sampling of signals consisting of a stream of pulses, covering the three different cases: periodic, finite and infinite streams of pulses. The criteria we consider for designing such systems are: a) Minimal sampling rate which allows perfect reconstruction, b) numerical stability (with sufficiently separated time delays), and c) minimal restrictions on the number of pulses per sampling period.

We begin by treating periodic pulse streams. For this setting, we develop a general sampling scheme which allows to determine the times and amplitudes of the pulses, from a minimal number of samples. Assuming an arbitrary pulse shape, we derive a condition on the sampling kernel, under which the solution is guaranteed. As we show, previous work [3] is a special case of our extended results. In contrast to the infinite time-support of the filters in [3], we develop a compactly supported class of filters which satisfy our mathematical condition. This class of filters consists of a sum of sinc functions in the frequency domain. We therefore refer to such functions as *Sum of Sincs* (SoS). To the best of our knowledge, this is the first class of finite support filters that solve the periodic case.

The compact support of the SoS class, in contrast to the lowpass filter proposed in [3], is the key to extending the periodic solution to the finite stream case. Generalizing the

SoS class, we design a sampling and reconstruction scheme which perfectly reconstructs a finite stream of pulses from a minimal number of samples, as long as the pulse shape has compact support. Our reconstruction is numerically stable for both small values of  $L$  and large number of pulses, e.g.,  $L = 100$ . In contrast, Gaussian sampling filters [3], [11] are unstable for  $L > 9$ , and we show in simulations that the moments approach [12] exhibits large estimation errors for  $L \geq 5$ . In addition, we demonstrate substantial improvement in noise robustness even for low values of  $L$ . Our advantage stems from the fact that we propose compactly supported filters on the one hand, while staying within the regime of Fourier coefficients reconstruction on the other hand.

The compact support of the SoS class becomes advantageous when we extend our results to the infinite stream setting as well. In this context, we consider a signal consisting of pulse bursts, where within each burst there may be a large number of closely spaced pulses. We assume a maximal permitted density of the bursts, and design a sampling and reconstruction scheme which guarantees perfect reconstruction from low rate samples. The proposed method is based on our solution for the finite case, and therefore exhibits numerically stable reconstruction even for a large number of closely spaced pulses, which cannot be treated using existing approaches [12]. Another advantage is that in contrast to previous work, the constraints cast on the structure of the signal are independent of  $L$  (the number of pulses in each burst) and therefore similar sampling schemes may be used for different values of  $L$ . Finally, we show that our sampling scheme requires lower sampling rate for  $L \geq 3$ .

As an application, we demonstrate our finite stream sampling scheme on real ultrasound imaging data acquired by GE healthcare's ultrasound system. We obtain high accuracy estimation while reducing the required number of samples by 2 orders of magnitude in comparison with current imaging techniques.

The remainder of the paper is organized as follows. In Section II we present the periodic signal model, and derive a general sampling scheme. A specific class of filters (the SoS class) which satisfy this condition, and have compact support, is then developed and demonstrated via simulations. An extension of the SoS class to the finite case is presented in Section III, followed by simulations showing the advantages of our method in high order problems and in noisy settings. In Section IV, we present our sampling scheme for an infinite stream of pulses. Section V explores the relationships of our work with previous methods. Finally, in Section VI, we demonstrate our method on real ultrasound imaging data.

## II. PERIODIC STREAM OF PULSES

### A. Notations and Definitions

Matrices and vectors are denoted by bold font, with lowercase letters corresponding to vectors and uppercase letters to matrices. The  $n$ th element of a vector  $\mathbf{a}$  is written as  $\mathbf{a}_n$ , and  $\mathbf{A}_{ij}$  denotes the  $ij$ th element of a matrix  $\mathbf{A}$ . Superscripts  $(\cdot)^*$ ,  $(\cdot)^T$  and  $(\cdot)^H$  represent complex conjugation, transposition and conjugate transposition, respectively. The

Moore-Penrose pseudo-inverse of a matrix  $\mathbf{A}$  is written as  $\mathbf{A}^\dagger$ . The continuous-time Fourier transform (CTFT) of a continuous-time signal  $x(t) \in L_2$  is defined by  $X(\omega) = \int_{-\infty}^{\infty} x(t) e^{-j\omega t} dt$ , and

$$\langle x(t), y(t) \rangle = \int_{-\infty}^{\infty} x^*(t) y(t) dt, \quad (1)$$

denotes the inner product between two  $L_2$  signals.

### B. Problem Formulation

Consider a  $\tau$ -periodic stream of pulses, defined as

$$x(t) = \sum_{m \in \mathbb{Z}} \sum_{l=1}^L a_l h(t - t_l - m\tau), \quad (2)$$

where  $h(t)$  is a known pulse shape,  $\tau$  is the known period, and  $\{t_l, a_l\}_{l=1}^L$ ,  $t_l \in [0, \tau)$ ,  $a_l \in \mathbb{C}$ ,  $l = 1 \dots L$  are the unknown delays and amplitudes. Our goal is to sample  $x(t)$  and reconstruct it, from a minimal number of samples. Since the signal has  $2L$  degrees of freedom, we expect the minimal number of samples to be  $2L$ . We are primarily interested in pulses which have small time-support. Direct uniform sampling of  $2L$  samples of the signal will result in many zero samples, since the probability for the sample to hit a pulse is very low. Therefore, we must construct a more sophisticated sampling scheme.

Define the periodic continuation of  $h(t)$  as  $f(t) = \sum_{m \in \mathbb{Z}} h(t - m\tau)$ . Using Poisson's summation formula [14],  $f(t)$  may be written as

$$f(t) = \frac{1}{\tau} \sum_{k \in \mathbb{Z}} H\left(\frac{2\pi k}{\tau}\right) e^{j2\pi kt/\tau}, \quad (3)$$

where  $H(\omega)$  denotes the CTFT of the pulse  $h(t)$ . Substituting (3) into (2) we obtain

$$\begin{aligned} x(t) &= \sum_{l=1}^L a_l f(t - t_l) \\ &= \sum_{k \in \mathbb{Z}} \left( \frac{1}{\tau} H\left(\frac{2\pi k}{\tau}\right) \sum_{l=1}^L a_l e^{-j2\pi kt_l/\tau} \right) e^{j2\pi kt/\tau} \\ &= \sum_{k \in \mathbb{Z}} X[k] e^{j2\pi kt/\tau}, \end{aligned} \quad (4)$$

where we denoted

$$X[k] = \frac{1}{\tau} H\left(\frac{2\pi k}{\tau}\right) \sum_{l=1}^L a_l e^{-j2\pi kt_l/\tau}. \quad (5)$$

The expansion in (4) is the Fourier series representation of the  $\tau$ -periodic signal  $x(t)$  with Fourier coefficients given by (5).

We will now show that once  $2L$  or more Fourier coefficients of  $x(t)$  are known, we may use conventional tools from spectral analysis in order to determine the unknowns  $\{t_l, a_l\}_{l=1}^L$ . The method by which the Fourier coefficients are obtained will be presented in subsequent sections.

Define a set  $\mathcal{K}$  of  $M$  consecutive indices such that  $H\left(\frac{2\pi k}{\tau}\right) \neq 0, \forall k \in \mathcal{K}$ . We assume such a set exists, which is usually the case for short time-support pulses  $h(t)$ . Denote

by  $\mathbf{H}$  the  $M \times M$  diagonal matrix with  $k$ th entry  $\frac{1}{\tau} H\left(\frac{2\pi k}{\tau}\right)$ , and by  $\mathbf{V}(\mathbf{t})$  the  $M \times L$  matrix with  $kl$ th element  $e^{-j2\pi kt_l/\tau}$ , where  $\mathbf{t} = \{t_1, \dots, t_L\}$  is the vector of the unknown delays. In addition denote by  $\mathbf{a}$  the length- $L$  vector whose  $l$ th element is  $a_l$ , and by  $\mathbf{x}$  the length- $M$  vector whose  $k$ th element is  $X[k]$ . We may then write (5) in matrix form as

$$\mathbf{x} = \mathbf{H}\mathbf{V}(\mathbf{t})\mathbf{a}. \quad (6)$$

Since  $\mathbf{H}$  is invertible by construction we define  $\mathbf{y} = \mathbf{H}^{-1}\mathbf{x}$ , which satisfies

$$\mathbf{y} = \mathbf{V}(\mathbf{t})\mathbf{a}. \quad (7)$$

The matrix  $\mathbf{V}$  is a Vandermonde matrix and therefore has full column rank [10], [15] as long as  $M \geq L$  and the time-delays are distinct, i.e.,  $t_i \neq t_j$  for all  $i \neq j$ .

Writing the expression for the  $k$ th element of the vector  $\mathbf{y}$  in (7) explicitly:

$$y_k = \sum_{l=1}^L a_l e^{-j2\pi kt_l/\tau}. \quad (8)$$

Evidently, given the vector  $\mathbf{x}$ , (7) is a standard problem of finding the frequencies and amplitudes of a sum of  $L$  complex exponentials (see [10] for a review of this topic). This problem may be solved as long as  $|\mathcal{K}| = M \geq 2L$ .

The annihilating filter approach used extensively by Vetterli et al. [3], [9] is one way of recovering the frequencies. This method can solve the problem using the critical number of samples  $M = 2L$ , as opposed to other techniques such as MUSIC [16], [17] and ESPRIT [18] which require substantial oversampling. Since we are interested in minimal-rate sampling, we use the annihilating filter method throughout the paper.

### C. Obtaining The Fourier Series Coefficients

As we have seen, given the vector of  $M \geq 2L$  Fourier series coefficients  $\mathbf{x}$ , we may use standard tools from spectral analysis (e.g., annihilating filter) to determine the set  $\{t_l, a_l\}_{l=1}^L$ . In practice, however, the signal is sampled in the time domain, and therefore we do not have direct access to samples of  $\mathbf{x}$ . Our goal now is to design a single-channel sampling scheme which will allow to obtain the vector  $\mathbf{x}$  from time-domain samples. In contrast to previous work regarding the periodic case [3], [9] which focused on a low-pass sampling filter, in this section we derive a general condition on the sampling kernel allowing to obtain the vector  $\mathbf{x}$ , and consequently recover the time-delays  $\mathbf{t}$  and the amplitudes  $\mathbf{a}$ . For the sake of clarity we confine ourselves to uniform sampling, but these results extend in a straightforward manner to nonuniform sampling as well.

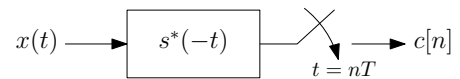


Fig. 1. Single channel sampling scheme.

Consider sampling the signal  $x(t)$  uniformly with sampling kernel  $s^*(-t)$  and sampling period  $T$ , as depicted in Fig. 1.

The samples are given by

$$c[n] = \int_{-\infty}^{\infty} x(t)s^*(t-nT)dt = \langle s(t-nT), x(t) \rangle. \quad (9)$$

Substituting (4) into (9) we have

$$\begin{aligned} c[n] &= \sum_{k \in \mathbb{Z}} X[k] \int_{-\infty}^{\infty} e^{j2\pi kt/\tau} s^*(t-nT)dt \\ &= \sum_{k \in \mathbb{Z}} X[k] e^{j2\pi knT/\tau} \int_{-\infty}^{\infty} e^{j2\pi kt/\tau} s^*(t)dt \\ &= \sum_{k \in \mathbb{Z}} X[k] e^{j2\pi knT/\tau} S^*(2\pi k/\tau), \end{aligned} \quad (10)$$

where  $S(\omega)$  is the CTFT of  $s(t)$ . Choosing any filter  $s^*(-t)$  which satisfies

$$S^*(\omega) = \begin{cases} 0 & \omega = 2\pi k/\tau, k \notin \mathcal{K} \\ \text{nonzero} & \omega = 2\pi k/\tau, k \in \mathcal{K} \\ \text{arbitrary} & \text{otherwise,} \end{cases} \quad (11)$$

we can rewrite (10) as

$$c[n] = \sum_{k \in \mathcal{K}} X[k] e^{j2\pi knT/\tau} S^*(2\pi k/\tau). \quad (12)$$

In contrast to (10), the sum in (12) is finite. Note that (11) implies that any real filter meeting this condition will satisfy  $k \in \mathcal{K} \Rightarrow -k \in \mathcal{K}$ , and in addition  $S(2\pi k/\tau) = S^*(-2\pi k/\tau)$ , due to the conjugate symmetry of real filters.

Defining the  $M \times M$  diagonal matrix  $\mathbf{S}$  whose  $k$ th entry is  $S^*(2\pi k/\tau)$  for all  $k \in \mathcal{K}$ , and the length- $N$  vector  $\mathbf{c}$  whose  $n$ th element is  $c[n]$ , we may write (12) as

$$\mathbf{c} = \mathbf{V}(-\mathbf{t}_s)\mathbf{S}\mathbf{x} \quad (13)$$

where  $\mathbf{t}_s = \{nT : n = 0 \dots N-1\}$ , and  $\mathbf{V}$  is defined as in (6) with a different parameter  $-\mathbf{t}_s$  and dimensions  $N \times M$ . The matrix  $\mathbf{S}$  is invertible by construction. Since  $\mathbf{V}$  is Vandermonde, it is left invertible as long as  $N \geq M$ . Therefore,

$$\mathbf{x} = \mathbf{S}^{-1}\mathbf{V}^\dagger(-\mathbf{t}_s)\mathbf{c}. \quad (14)$$

In the special case where  $N = M$  and  $T = \tau/N$ , the recovery in (14) becomes:

$$\mathbf{x} = \mathbf{S}^{-1}\text{DFT}\{\mathbf{c}\}, \quad (15)$$

i.e., the vector  $\mathbf{x}$  is obtained by applying the Discrete Fourier Transform (DFT) on the sample vector, followed by a correction matrix related to the sampling filter.

The idea behind this sampling scheme is that each sample is actually a linear combination of the elements of  $\mathbf{x}$ . The sampling kernel  $s^*(-t)$  is designed to pass the coefficients  $X[k]$ ,  $k \in \mathcal{K}$  while suppressing all other coefficients  $X[k]$ ,  $k \notin \mathcal{K}$ . This is exactly what the condition in (11) means. This sampling scheme guarantees that each sample combination is linearly independent of the others. Therefore, the linear system of equations in (13) has full column rank which allows us to solve for the vector  $\mathbf{x}$ .

We summarize this result in the following theorem.

**Theorem 1.** Consider the  $\tau$ -periodic stream of pulses of order  $L$ :

$$x(t) = \sum_{m \in \mathbb{Z}} \sum_{l=1}^L a_l h(t - t_l - m\tau).$$

Choose a set  $\mathcal{K}$  of consecutive indices for which  $H(2\pi k/\tau) \neq 0$ ,  $\forall k \in \mathcal{K}$ . Then the samples

$$c[n] = \langle s(t-nT), x(t) \rangle, \quad n = 0 \dots N-1,$$

uniquely determine the signal  $x(t)$  for any filter  $s^*(-t)$  satisfying condition (11), as long as  $N \geq |\mathcal{K}| \geq 2L$ .

In order to extend Theorem 1 to nonuniform sampling, we only need to substitute the nonuniform sampling times in the vector  $\mathbf{t}_s$  in (14).

Theorem 1 presents a general single channel sampling scheme. One special case of this framework is the one proposed by Vetterli et al. in [3] in which  $s^*(-t) = B \text{sinc}(-Bt)$ , where  $B = M/\tau$  and  $N \geq M \geq 2L$ . In this case  $s(t)$  is an ideal low-pass filter of bandwidth  $B$  with

$$S(\omega) = \text{rect}\left(\frac{\omega}{2\pi}\right). \quad (16)$$

Clearly, (16) satisfies the general condition in (11) with  $\mathcal{K} = \{-\lfloor M/2 \rfloor, \dots, \lfloor M/2 \rfloor\}$  and  $S\left(\frac{2\pi k}{\tau}\right) = 1$ ,  $\forall k \in \mathcal{K}$ . Note that since this filter is real valued it must satisfy  $k \in \mathcal{K} \Rightarrow -k \in \mathcal{K}$ , i.e., the indices come in pairs except for  $k = 0$ . Since  $k = 0$  is part of the set  $\mathcal{K}$ , in this case the cardinality  $M = |\mathcal{K}|$  must be odd valued so that  $N \geq M \geq 2L + 1$  samples, rather than the minimal rate  $N \geq 2L$ .

The ideal low-pass filter is bandlimited, and therefore has infinite time-support. Due to the infinite support of the filter it cannot be extended to finite and infinite streams of pulses. In the next section we propose a class of non-bandlimited sampling kernels, which exploit the additional degrees of freedom in condition (11), and have compact support in the time domain. The compact support allows us to extend this class to finite and infinite streams, presented in Sections III and IV, respectively. While the work in [12] focused on finite support filters, their reconstruction scheme is based on moments of the signal, rather than Fourier coefficients, and therefore the sampling kernels do not satisfy (11). As we demonstrate in the following sections, our method is advantageous in both high order problems and noisy scenarios, in which the moment method becomes very sensitive.

#### D. Compactly Supported Sampling Kernels

Consider the following class of functions, which we call the SoS class since it consists of a sum of sincs in the frequency domain:

$$G(\omega) = \frac{\tau}{\sqrt{2\pi}} \sum_{k \in \mathcal{K}} b_k \text{sinc}\left(\frac{\omega}{2\pi/\tau} - k\right) \quad (17)$$

where  $b_k \neq 0$ ,  $k \in \mathcal{K}$ . The filter in (17) is real valued if and only if  $k \in \mathcal{K} \Rightarrow -k \in \mathcal{K}$  and  $b_k = b_{-k}^*$  for all  $k \in \mathcal{K}$ . Since for each sinc in the sum

$$\text{sinc}\left(\frac{\omega}{2\pi/\tau} - k\right) = \begin{cases} 1 & \omega = 2\pi k'/\tau, k' = k \\ 0 & \omega = 2\pi k'/\tau, k' \neq k \end{cases}, \quad (18)$$

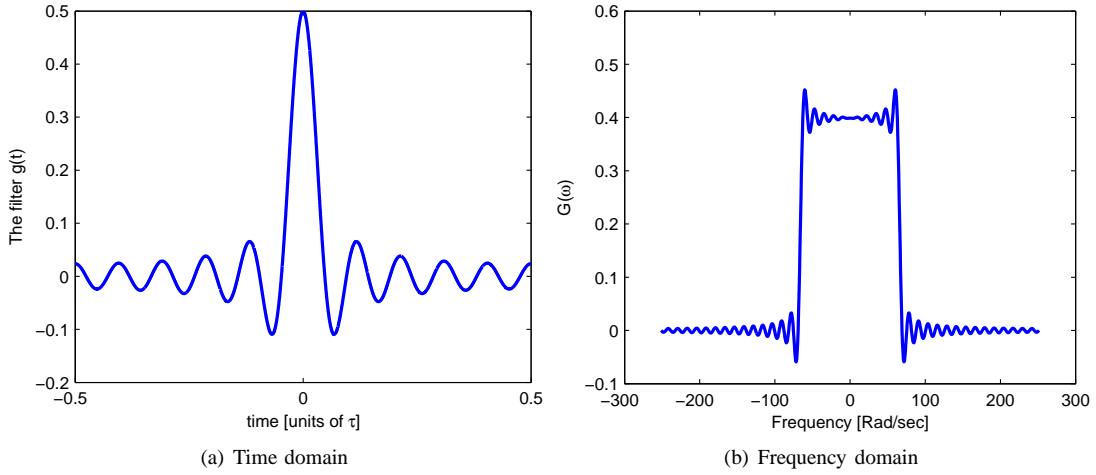


Fig. 2. The filter  $g(t)$  with all coefficients  $b_k = 1$ .

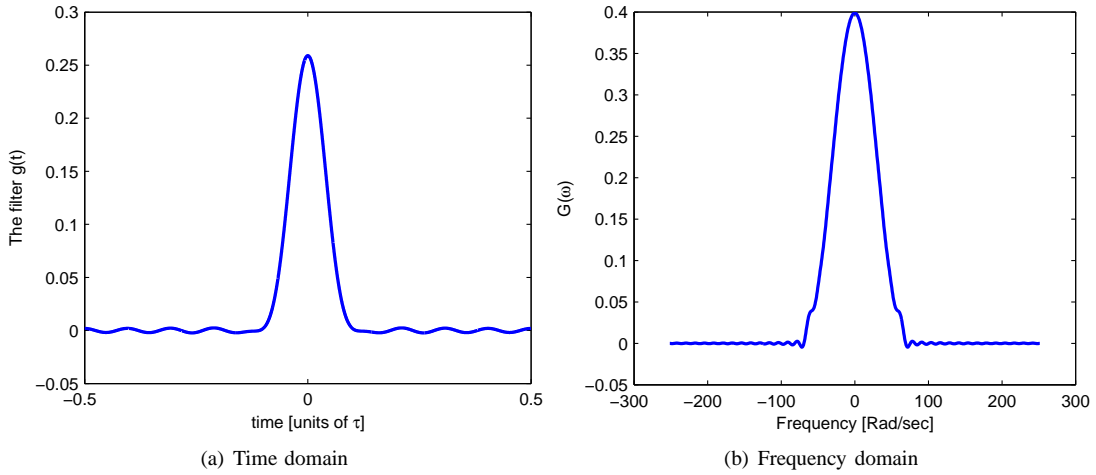


Fig. 3. The filter  $g(t)$  with hamming window coefficients.

the filter  $G(\omega)$  satisfies (11) by construction. Switching to the time domain

$$g(t) = \text{rect}\left(\frac{t}{\tau}\right) \sum_{k \in \mathcal{K}} b_k e^{j2\pi kt/\tau}, \quad (19)$$

which is clearly a time compact filter with support  $\tau$ .

The SoS class in (19) may be extended to a more general structure

$$G(\omega) = \frac{\tau}{\sqrt{2\pi}} \sum_{k \in \mathcal{K}} b_k \phi\left(\frac{\omega}{2\pi/\tau} - k\right) \quad (20)$$

where  $b_k \neq 0$ ,  $k \in \mathcal{K}$ , and  $\phi(\omega)$  is any function satisfying:

$$\phi(\omega) = \begin{cases} 1 & \omega = 0 \\ 0 & |\omega| \in \mathbb{N} \\ \text{arbitrary} & \text{otherwise} \end{cases}. \quad (21)$$

This more general structure allows for smooth versions of the rect function, which is important when practically implementing analog filters.

The function  $g(t)$  represents a class of filters determined by the parameters  $\{b_k\}_{k \in \mathcal{K}}$ . These degrees of freedom offer a filter design tool where the free parameters  $\{b_k\}_{k \in \mathcal{K}}$  may

be optimized for different goals, e.g., parameters which will result in a feasible analog filter.

Determining the parameters  $\{b_k\}_{k \in \mathcal{K}}$  may be viewed from a more empirical point of view. The impulse response of any analog filter having support  $\tau$  may be written in terms of a windowed Fourier series as

$$\Phi(t) = \text{rect}\left(\frac{t}{\tau}\right) \sum_{k \in \mathbb{Z}} \beta_k e^{j2\pi kt/\tau}. \quad (22)$$

Confining ourselves to filters which satisfy  $\beta_k \neq 0$ ,  $k \in \mathcal{K}$ , we may truncate the series and choose:

$$b_k = \begin{cases} \beta_k & k \in \mathcal{K} \\ 0 & k \notin \mathcal{K} \end{cases} \quad (23)$$

as the parameters of  $g(t)$  in (19). With this choice,  $g(t)$  can be viewed as an approximation to  $\Phi(t)$ . Notice that there is an inherent tradeoff here: using more coefficients will result in a better approximation of the analog filter, but in turn will require more samples, since the number of samples  $N$  must be greater than the cardinality of the set  $\mathcal{K}$ .

To demonstrate the filter  $g(t)$  we first choose  $\mathcal{K} =$

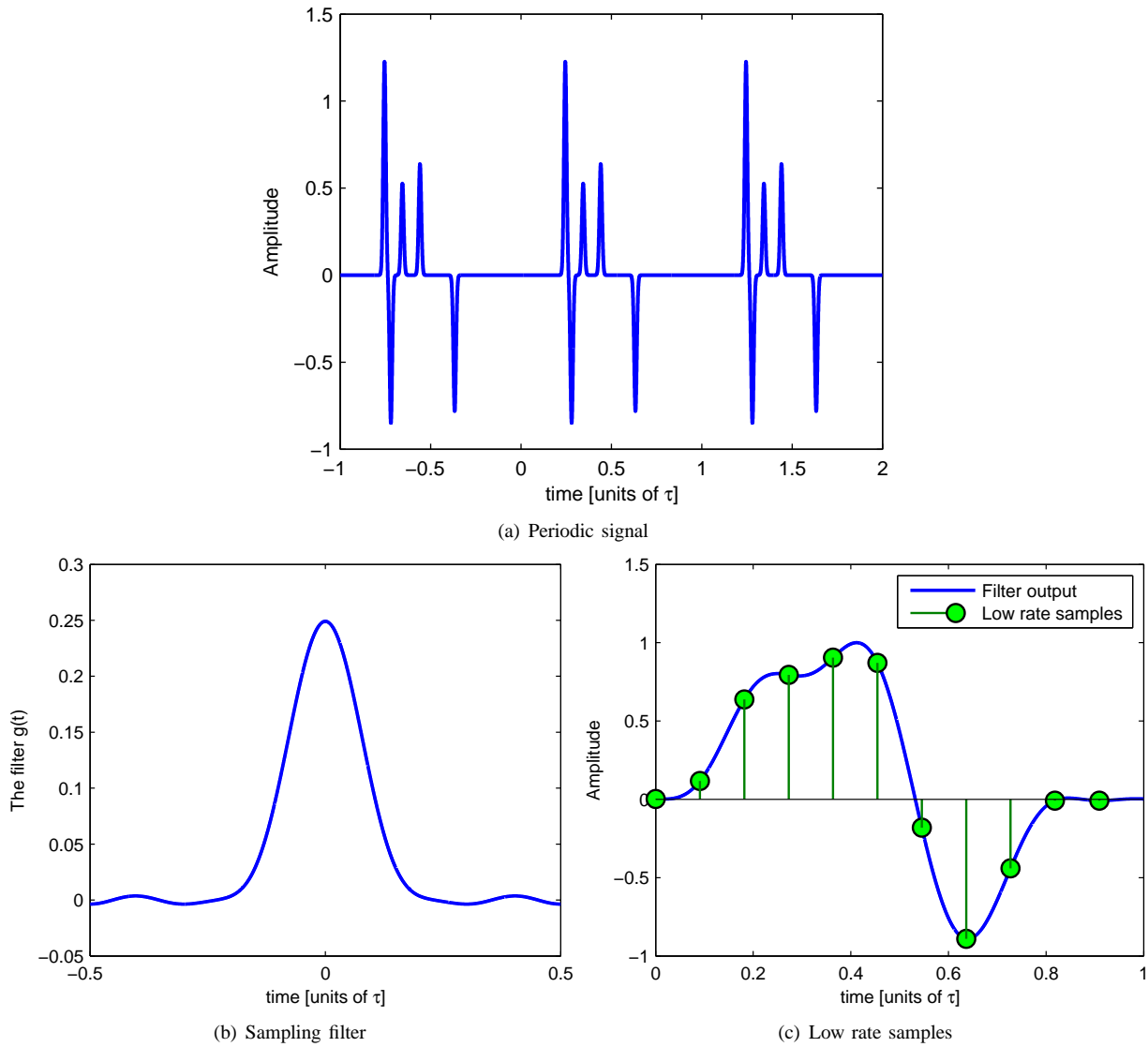


Fig. 4. From an analog signal to low rate samples (a) Original periodic signal,  $x(t)$ , which consists of 5 Gaussians (3 periods are shown). (b) Sampling filter. (c) Low rate samples depicted over the filtered signal.

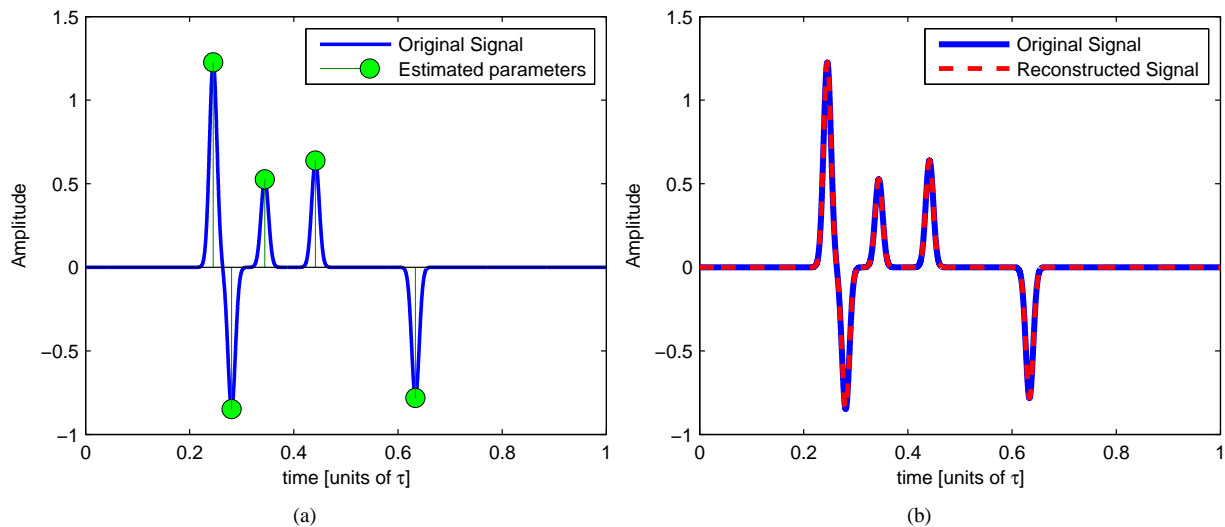


Fig. 5. (a) Estimated time-delays and amplitudes depicted over the original signal. (b) Reconstructed signal vs. original one. The reconstruction is exact to numerical precision.

$\{-p, \dots, p\}$  and set all coefficients  $\{b_k\}$  to one, resulting in

$$g(t) = \text{rect}\left(\frac{t}{\tau}\right) \sum_{k=-p}^p e^{j2\pi kt/\tau} = \text{rect}\left(\frac{t}{\tau}\right) D_p(2\pi t/\tau), \quad (24)$$

where the Dirichlet kernel  $D_p(t)$  is defined by

$$D_p(t) = \sum_{k=-p}^p e^{jkt} = \frac{\sin((p + \frac{1}{2})t)}{\sin(t/2)}. \quad (25)$$

The resulting filter for  $p = 10$  and  $\tau = 1$  sec, is depicted in Fig. 2.

In Fig. 3 we show a different choice of  $g(t)$  where the  $b_k$ 's are chosen as a length- $M$  symmetric Hamming window:

$$b_k = 0.54 - 0.46 \cos\left(2\pi \frac{k + \lfloor M/2 \rfloor}{M}\right), \quad k \in \mathcal{K}. \quad (26)$$

Notice that in both cases the coefficients satisfy  $b_k = b_{-k}^*$ , and therefore, the resulting filters are real valued.

### E. Simulations

1) *Demonstration of Our Sampling and Reconstruction Scheme:* We begin with demonstrating our sampling scheme. The input signal  $x(t)$  consists of  $L = 5$  delayed and weighted versions of a Gaussian pulse  $h(t)$

$$h(t) = \frac{1}{\sqrt{2\pi\sigma^2}} \exp(-t^2/2\sigma^2), \quad (27)$$

with parameter  $\sigma = 7 \cdot 10^{-3}$ , and period  $\tau = 1$ . The time-delays and amplitudes were chosen randomly. In order to demonstrate near-critical sampling we choose the set of indices  $\mathcal{K} = \{-L, \dots, L\}$  with cardinality  $M = |\mathcal{K}| = 2L + 1 = 11$ . We filter  $x(t)$  with  $g(t)$  defined in (19), where the coefficients  $b_k$ ,  $k \in \mathcal{K}$  were set to be the length- $M$  symmetric Hamming window given by (26). The output of the filter is sampled uniformly  $N$  times, with sampling period  $T = \tau/N$ , where  $N = M = 11$ . The sampling process is depicted in Fig. 4.

The Fourier series coefficients were obtained from the samples as described in (14). Finally, the time-delays and amplitudes were reconstructed using the annihilating filter spectral analysis method. The reconstructed and original signals are depicted in Fig. 5. The estimation and reconstruction are both exact to numerical precision.

2) *Noisy Case:* We now consider the case in which the samples are corrupted by noise. We compare our performance to the sinc filter method presented in [3], which has high noise robustness as long as the pulses are sufficiently spaced, and show that our method retains this robustness.

Our signal consists of  $L = 2$  pulses, where the pulse here was chosen as  $h(t) = \delta(t)$ . The period was set to  $\tau = 1$ ,  $\mathcal{K} = \{-2, \dots, 2\}$ , and  $N = M = 5$  samples were taken, sampled uniformly with sampling period  $T = \tau/N$ . The sampling kernel is  $g^*(-t)$  defined in (19), where all coefficients  $\{b_k\}$  were set to one. In our setup additive white Gaussian noise (AWGN) is added to the samples, i.e., our samples are given by  $\mathbf{y} = \mathbf{c} + \mathbf{n}$  where  $\mathbf{c}$  is the uncorrupted

vector of samples, and  $\mathbf{n}$  consists of independent zero-mean Gaussian variables with variance  $\sigma^2$ . We define the SNR as:

$$\text{SNR} = \frac{\frac{1}{N} \|\mathbf{c}\|_2^2}{\sigma^2}, \quad (28)$$

where  $\|\cdot\|_2$  denotes the  $l_2$ -norm. In our experiments the variance of the noise is set to give the desired SNR.

The simulation consists of 1000 experiments for each SNR, where in each experiment a new noise vector is created. The time-delays were chosen to be  $\mathbf{t} = \tau \cdot (1/3 \ 2/3)^T$  and the amplitudes were set to one. The time-delays and the amplitudes remain constant throughout the experiments. We define the error in time-delay estimation as the average over all experiments of  $\|\mathbf{t} - \hat{\mathbf{t}}\|_2^2$ , where  $\mathbf{t}$  and  $\hat{\mathbf{t}}$  denote the true and estimated time-delays, respectively, sorted in increasing order. In Fig. 6 we show the error as a function of SNR, for our method versus the sinc sampling kernel. Evidently, both

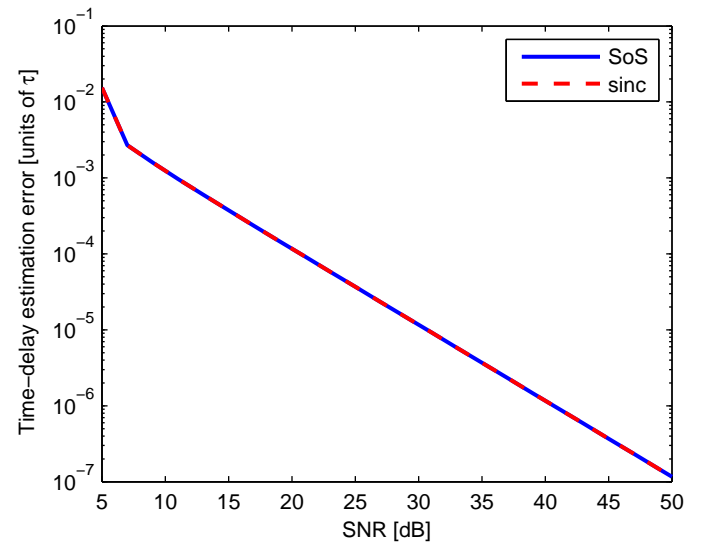


Fig. 6. Error in time-delay estimation as a function of SNR using our approach and the sinc filter method.

methods have the same performance. However our sampling scheme for the periodic case consists of sampling kernels having compact support in the time domain. In the next section we exploit the compact support of our filter, and extend the results to the finite stream case. We will show that our sampling and reconstruction scheme offers a numerically stable solution for this case, with high noise robustness.

Finally, we can improve reconstruction accuracy at the expense of oversampling, as illustrated in Fig. 7. Here we show recovery performance for oversampling factors of 2, 4 and 8.

## III. FINITE STREAM OF PULSES

### A. Extension of SoS Class

Consider now a finite stream of pulses, defined as

$$\tilde{x}(t) = \sum_{l=1}^L a_l h(t - t_l), \quad t_l \in [0, \tau), \quad a_l \in \mathbb{R}, \quad l = 1 \dots L, \quad (29)$$

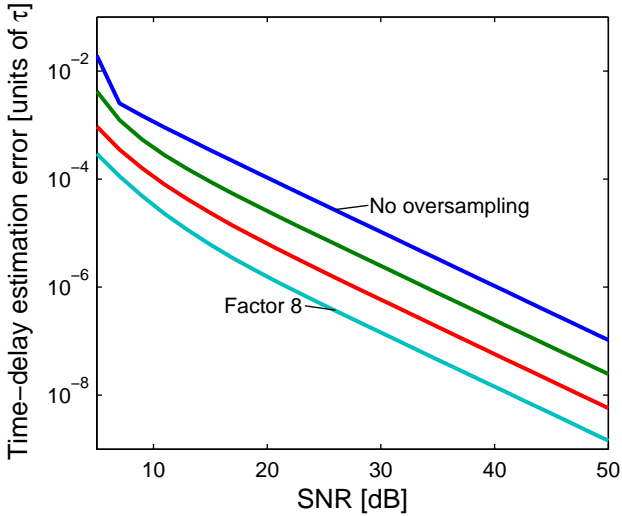


Fig. 7. The effect of oversampling on estimation error. Oversampling by a factor of 1, 2, 4 and 8.

where, as in Section II,  $h(t)$  is a known pulse shape, and  $\{t_l, a_l\}_{l=1}^L$  are the unknown delays and amplitudes. The time-delays  $\{t_l\}_{l=1}^L$  are restricted to lie in a finite time interval  $[0, \tau)$ . Again, there are only  $2L$  degrees of freedom, so we expect the critical number of samples to be  $2L$ . We wish to design a sampling and reconstruction method which perfectly reconstructs the signal  $\tilde{x}(t)$  from a minimal number of samples. In this section we assume that the pulse  $h(t)$  has finite support  $R$ , i.e.,

$$h(t) = 0, \forall |t| \geq R/2. \quad (30)$$

This is a rather weak condition, since our primary interest is in very short pulses which have wide, or even infinite, frequency support, and therefore cannot be sampled efficiently using classical sampling schemes for bandlimited signals.

Note that  $x(t)$  in (2) is the periodic continuation of  $\tilde{x}(t)$  in (29). Therefore,  $\tilde{x}(t)$  may be convolved with a Dirac comb to yield  $x(t)$ :

$$x(t) = \tilde{x}(t) * \sum_{m \in \mathbb{Z}} \delta(t - m\tau). \quad (31)$$

Exploiting this observation, we can write the samples of the periodic signal  $c[n]$  as

$$\begin{aligned} c[n] &= x(t) * g^*(-t) \Big|_{t=nT} \\ &= \tilde{x}(t) * \sum_{m \in \mathbb{Z}} \delta(t - m\tau) * g^*(-t) \Big|_{t=nT} \\ &= \tilde{x}(t) * \tilde{g}^*(-t) \Big|_{t=nT} \end{aligned} \quad (32)$$

where we denoted  $\tilde{g}(t) = \sum_{m \in \mathbb{Z}} g(t + m\tau)$ . In other words, sampling the periodic signal  $x(t)$  in (2) with a filter  $g^*(-t)$ , is equivalent to sampling the aperiodic signal  $\tilde{x}(t)$  with the filter  $\tilde{g}^*(-t)$  which is the periodic extension of  $g^*(-t)$ . Therefore, in order to obtain the exact same samples  $c[n]$ ,  $n = 0 \dots N-1$  as in (12) for the periodic case, we could sample  $\tilde{x}(t)$  with a periodic sampling kernel  $\tilde{g}^*(-t)$ . However, a periodic filter is of course impractical since it has infinite energy and infinite support. We now propose a variant of the above approach

which exploits the compact support of the filter  $g(t)$ , and under mild assumptions on the pulse  $h(t)$  obtains precisely the same samples  $c[n]$  as in the periodic case, while using a compactly supported filter.

From (10), and using  $g^*(-t)$  as the sampling kernel, the samples taken in the periodic case can be written as

$$\begin{aligned} c[n] &= \langle g(t - nT), x(t) \rangle \\ &= \sum_{m \in \mathbb{Z}} \sum_{l=1}^L a_l \int_{-\infty}^{\infty} h(t - t_l - m\tau) g^*(t - nT) dt \\ &= \sum_{m \in \mathbb{Z}} \sum_{l=1}^L a_l \int_{-\infty}^{\infty} h(t) g^*(t - (nT - t_l - m\tau)) dt \\ &= \sum_{m \in \mathbb{Z}} \sum_{l=1}^L a_l \varphi(nT - t_l - m\tau), \end{aligned} \quad (33)$$

where we defined

$$\varphi(\vartheta) = \langle g(t - \vartheta), h(t) \rangle. \quad (34)$$

Since  $g(t)$  in (19) vanishes for all  $|t| > \tau/2$  and  $h(t)$  satisfies (30), the support of  $\varphi(t)$  is  $(R + \tau)$ , i.e.,

$$\varphi(t) = 0 \quad \text{for all } |t| \geq (R + \tau)/2. \quad (35)$$

Using this property, the summation in (33) will be over nonzero values for indices  $m$  satisfying

$$|nT - t_l - m\tau| < (R + \tau)/2. \quad (36)$$

Sampling within the window  $[0, \tau)$ , i.e.,  $nT \in [0, \tau)$ , and noting that the time-delays lie in the interval  $t_l \in [0, \tau)$ ,  $l = 1 \dots L$ , (36) implies that

$$(R + \tau)/2 > |nT - t_l - m\tau| \geq |m|\tau - |nT - t_l| > (|m| - 1)\tau. \quad (37)$$

Here we used the triangle inequality and the fact that  $|nT - t_l| < \tau$  in our setting. Therefore,

$$|m| < \frac{R/\tau + 3}{2} \Rightarrow |m| \leq \left\lfloor \frac{R/\tau + 3}{2} \right\rfloor - 1 \triangleq r, \quad (38)$$

i.e., the elements of the sum in (33) vanish for all  $m$  but the values in (38). Consequently, the infinite sum in (33) reduces to a finite sum over  $m \leq |r|$  so that (33) becomes

$$\begin{aligned} c[n] &= \sum_{m=-r}^r \sum_{l=1}^L a_l \varphi(nT - t_l - m\tau) \\ &= \sum_{m=-r}^r \sum_{l=1}^L a_l \int_{-\infty}^{\infty} h(t - t_l) g^*(t - nT + m\tau) dt \\ &= \left\langle \sum_{m=-r}^r g(t - nT + m\tau), \sum_{l=1}^L a_l h(t - t_l) \right\rangle, \end{aligned} \quad (39)$$

where in the last equality we used the linearity of the inner product. Defining a function which consists of  $(2r+1)$  periods of  $g(t)$ :

$$g_r(t) = \sum_{m=-r}^r g(t + m\tau), \quad (40)$$

we conclude that

$$c[n] = \langle g_r(t - nT), \tilde{x}(t) \rangle. \quad (41)$$

Therefore, the samples  $c[n]$  can be obtained by filtering the aperiodic signal  $\tilde{x}(t)$  with the filter  $g_r^*(-t)$  prior to sampling. This filter, in contrast to  $\tilde{g}(t)$  in (32), has compact support equal to  $(2r + 1)\tau$ .

We summarize this result in the following theorem.

**Theorem 2.** Consider the finite stream of pulses given by:

$$\tilde{x}(t) = \sum_{l=1}^L a_l h(t - t_l), \quad t_l \in [0, \tau), \quad a_l \in \mathbb{R},$$

where  $h(t)$  has finite support  $R$ . Choose a set  $\mathcal{K}$  of consecutive indices for which  $H(2\pi k/\tau) \neq 0, \forall k \in \mathcal{K}$ . Then,  $N$  samples given by:

$$c[n] = \langle g_r(t - nT), \tilde{x}(t) \rangle, \quad n = 0 \dots N - 1, \quad nT \in [0, \tau),$$

where  $r$  is defined in (38) and  $g_r(t)$  is defined by (40) and compactly supported, uniquely determine the signal  $\tilde{x}(t)$  as long as  $N \geq |\mathcal{K}| \geq 2L$ .

If, for example, the support  $R$  of  $h(t)$  satisfies  $R \leq \tau$  then we obtain from (38) that  $r = 1$ . Therefore, the filter in this case would consist of 3 periods of  $g(t)$ :

$$g_{3p}(t) \triangleq g_r(t)|_{r=1} = g(t - \tau) + g(t) + g(t + \tau). \quad (42)$$

Practical implementation of the filter may be carried out using delay-lines.

The problem of sampling and reconstructing a finite stream of pulses as in (29), has already been addressed in [3]. The pulse considered there is  $h(t) = \delta(t)$ . The authors use a Gaussian sampling kernel prior to sampling and reconstruction is based on the infinitely long tails of the Gaussian kernel. Although analytically exact, this method is numerically unstable as mentioned in [11]. This is due to the fact that the tails of the Gaussian consist of very small values, which leads to numerical instability. The authors of [11] propose improvements of this method, based on substantial oversampling, which lead to better performance, however for high order problems they still exhibit instability.

An alternative approach based on estimating the signal moments was proposed in [12]. This allows for compactly supported filters to be used in the sampling scheme, and therefore offers a local reconstruction scheme. With a proper choice of the sampling period, the minimal number of samples is sufficient for this method. However, the authors mention that high order problems lead to numerical instability. In contrast to the estimation of Fourier coefficients, estimating high order moments from the samples is unstable since unstable weighting of the samples is carried out during the process. We will show in simulations that in the presence of noise, even in low order problems, the performance of this method is inferior to the scheme we introduced here.

The strength of our reconstruction scheme is that we use a compactly supported filter, while staying within the regime of Fourier reconstruction. This allows us to stably solve high order problems, and achieve better noise robustness.

## B. Simulations

1) *Demonstration of the Sampling Scheme:* The input signal  $\tilde{x}(t)$  consists of  $L = 5$  delayed and weighted versions of the pulse  $h(t) = \delta(t)$ . The delays and weights were chosen randomly. We choose  $\mathcal{K} = \{-L, \dots, L\}$ , so that  $M = |\mathcal{K}| = 11$ . Since the support of  $h(t)$  satisfies  $R \leq \tau$  the parameter  $r$  in (38) equals 1, and therefore we filter  $\tilde{x}(t)$  with  $g_{3p}(t)$  defined in (42). The coefficients  $b_k, k \in \mathcal{K}$  were all set to one. The output of the filter is sampled uniformly  $N$  times, with sampling period  $T = \tau/N$ , where  $N = M = 11$ . Perfect reconstruction is achieved as can be seen in Fig. 8.

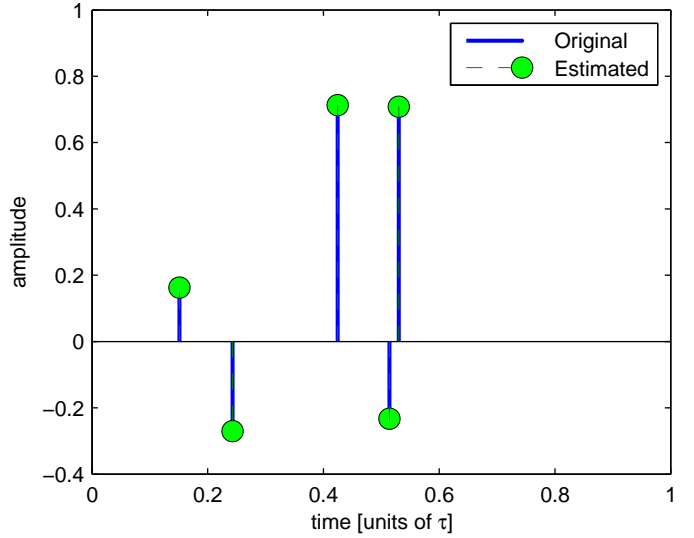


Fig. 8. Application of the filter  $g_{3p}(t)$  on a finite stream of  $L = 5$  diracs.

The estimation is exact to numerical precision.

2) *High Order Problems:* The same simulation was carried out with  $L = 20$  diracs. The results are shown in Fig. 9. Here again, the reconstruction is perfect even for this high order problem.

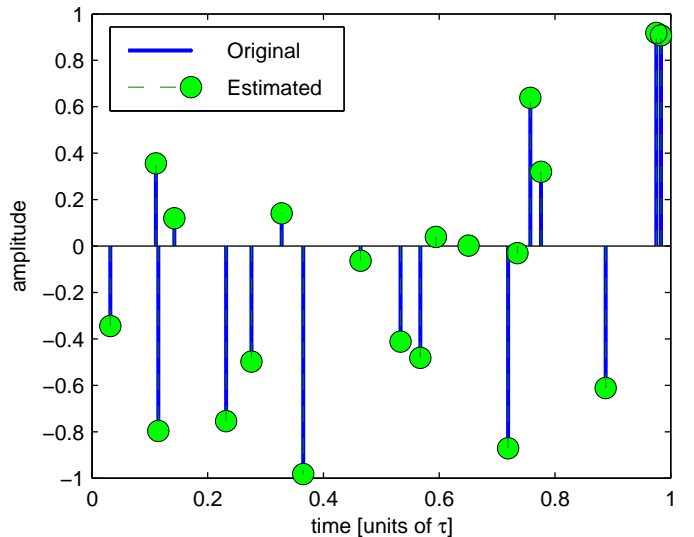


Fig. 9. High order problems: application of the filter  $g_{3p}(t)$  on a finite stream of  $L = 20$  diracs.

3) *Noisy Case*: We now examine the performance of our method in the presence of noise. In addition, we compare our performance to the one proposed in [12], using B-spline filters, and to the Gaussian sampling kernel suggested in [3]. The signal consists of  $L = 2$  diracs. The time-delays are set to be  $\mathbf{t} = \tau \cdot (1/3 \ 2/3)^T$ , where  $\tau = 1$ , and both amplitudes are one. The set of indices is  $\mathcal{K} = \{-L, \dots, L\}$ , and the number of samples is  $N = 5$ . The sampling period is  $T = \tau/N$ .

The method of noise corruption is the same as in Section II-E2. The B-splines we used were of order  $2L-1$ , and the sampling period,  $T$ , is the same as above. Hard thresholding was implemented in order to improve the spline method, as suggested by the authors in [12]. The threshold was chosen to be  $3\sigma_N$ , where  $\sigma_N$  is the standard deviation of the AWGN. For the Gaussian sampling kernel the parameter  $\sigma$  was optimized and took on the value of 0.25. The results are given in Fig. 10a. On average, our method outperforms the B-spline method by an order of magnitude. The performance of the Gaussian and the SoS approaches coincides for high SNR, but for low SNR the latter prevails.

In Fig. 10b-d the same simulation was carried out for  $L = 3, 5, 20$ , respectively<sup>1</sup>. Evidently, as  $L$  grows the advantage of our method becomes more substantial. For  $L \geq 5$  the spline method exhibits large estimation errors (on the order of  $\tau$ ), and the Gaussian kernel's performance exhibits degradation of 2-4 orders of magnitude comparing to the SoS filter. We have seen in simulations that for  $L \geq 6$  the Gaussian method shows numerical instability as well, leading to errors on the order of  $\tau$ . In contrast, our method estimates the time-delays stably, and with high noise robustness, as can be seen in Fig. 10d. The improved version of the Gaussian approach presented in [11] would not perform better in this high order case, since it fails for values of  $L > 9$ , as mentioned by the authors. The computational complexity of all methods is the same, since the main computational burden is the annihilating filter stage which is common to all techniques.

In the next section we extend the finite case results to an infinite stream of pulses. This can be done due to the compact support of our filter.

#### IV. INFINITE STREAM OF PULSES

##### A. Sampling And Reconstruction Scheme

We now consider the case of an infinite stream of pulses

$$z(t) = \sum_{l \in \mathbb{Z}} a_l h(t - t_l), \quad t_l, a_l \in \mathbb{R}. \quad (43)$$

We assume that the infinite signal has a bursty character, i.e., the signal has two distinct phases: a) bursts of maximal duration  $\tau$  containing at most  $L$  pulses, and b) quiet phases between bursts. For the sake of clarity we begin with the case  $h(t) = \delta(t)$ . For this choice the filter  $g_r^*(-t)$  in (40) reduces to  $g_{3p}^*(-t)$  of (42).

Since the filter  $g_{3p}^*(-t)$  has compact support  $3\tau$  we are assured that the current burst cannot influence samples taken  $3\tau/2$  seconds before or after it. In the finite case we have

<sup>1</sup>The parameter  $\sigma$  for the Gaussian method took on the values  $\sigma = 0.28, 0.32, 0.9$ , respectively.

confined ourselves to sampling within the interval  $[0, \tau)$ . Similarly, here, we assume that the samples are taken during the burst duration. Therefore, if the minimal spacing between any two consecutive bursts is  $3\tau/2$ , then we are guaranteed that each sample taken during the burst is influenced by one burst only, as depicted in Fig. 11. Consequently, the infinite problem can be reduced to a sequential solution of local distinct finite order problems, as in Section III. Here the compact support of our filter comes into play, allowing us to apply local reconstruction methods.

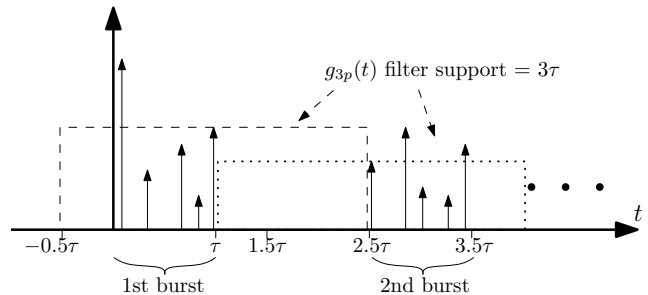


Fig. 11. Bursty signal  $z(t)$ . Spacing of  $3\tau/2$  between bursts ensures that the influence of the current burst ends before taking the samples of the next burst. This is due to the finite support,  $3\tau$  of the sampling kernel  $g_{3p}^*(-t)$ .

In the above argument we assume we know the locations of the bursts, since we must acquire samples from within the burst duration. Samples outside the burst duration are contaminated by energy from adjacent bursts. Nonetheless, knowledge of burst locations is available in many applications such as synchronized communication where the receiver knows when to expect the bursts, or in radar or imaging scenarios where the transmitter is itself the receiver.

We now state this result in a theorem.

**Theorem 3.** Consider a signal  $z(t)$  which is a stream of bursts consisting of delayed and weighted diracs. The maximal burst duration is  $\tau$ , and the maximal number of pulses within each burst is  $L$ . Then, the samples given by

$$c[n] = \langle g_{3p}(t - nT), z(t) \rangle, \quad n \in \mathbb{Z}$$

where  $g_{3p}(t)$  is defined by (42), are a sufficient characterization of  $z(t)$  as long as the spacing between two adjacent bursts is greater than  $3\tau/2$ , and the burst locations are known.

Extending this result to a general pulse  $h(t)$  is quite straightforward, as long as  $h(t)$  is compactly supported with support  $R$ , and we filter with  $g_r^*(-t)$  as defined in (40) with the appropriate  $r$  from (38). If we can choose a set  $\mathcal{K}$  of consecutive indices for which  $H(2\pi k/\tau) \neq 0, \forall k \in \mathcal{K}$  and we are guaranteed that the minimal spacing between two adjacent bursts is greater than  $((2r + 1)\tau + R)/2$ , then the above theorem holds.

#### V. RELATED WORK

Throughout the paper we mentioned closely related methods for sampling of pulse streams. In this section we explore in more detail the relationships between our approach and previously developed solutions proposed in [3], [9], [12], [13].

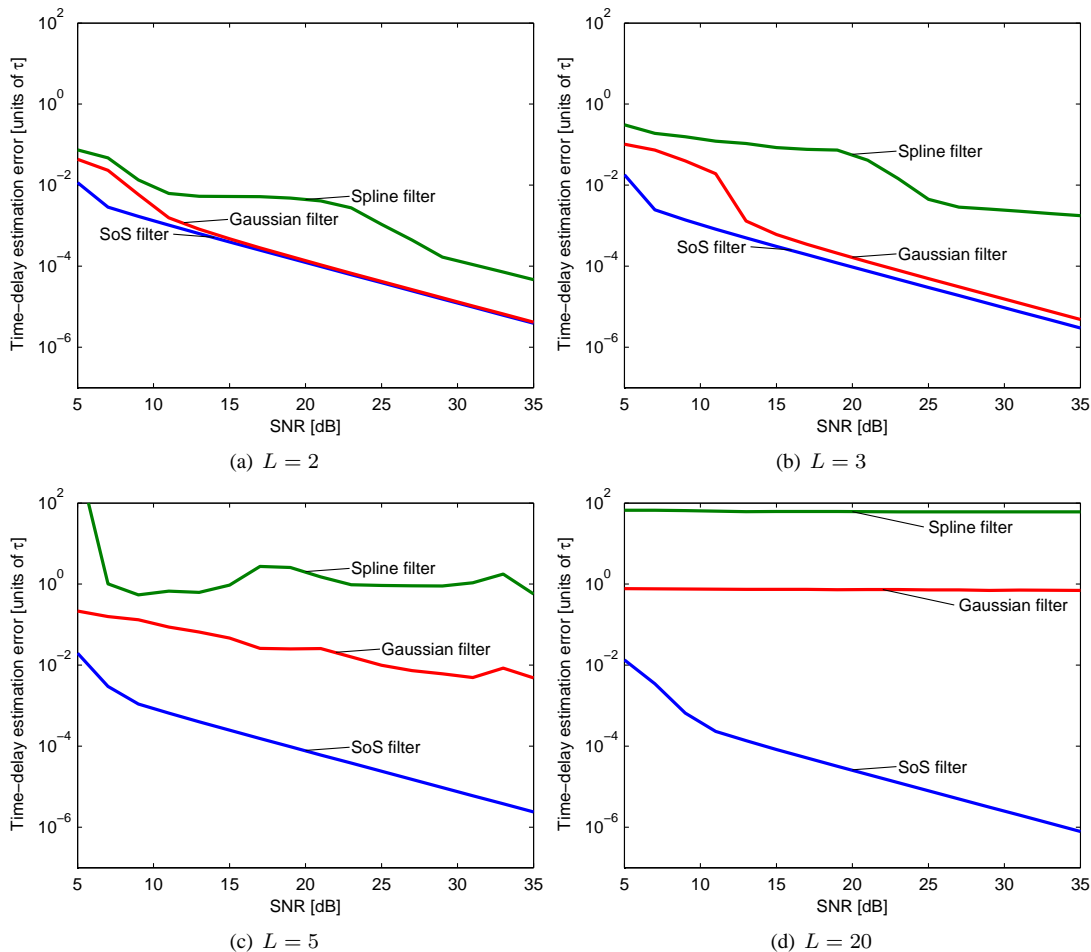


Fig. 10. Performance in the presence of noise: finite stream case. Our method vs. spline [12] and Gaussian [3] sampling kernels. (a)  $L = 2$  dirac pulses are present, (b)  $L = 3$  pulses, (c) high value of  $L = 5$  pulses, and (d) the performance for a very high value of  $L = 20$ .

### A. Periodic Case

The work in [3] was the first to address efficient sampling of pulse streams, e.g., diracs. Their approach for solving the periodic case was ideal lowpass filtering, followed by uniform sampling, which allowed to obtain the Fourier series coefficients of the signal. These coefficients are then processed by the annihilating filter to obtain the unknown time-delays and amplitudes. In Section II, we derived a general condition on the sampling kernel (11), under which recovery is guaranteed. The lowpass filter scheme of [3] is a special case of this result. The noise robustness of both the lowpass approach and our more general method is high as long as the pulses are well separated, since reconstruction from Fourier series coefficients is stable in this case.

The lowpass filter is bandlimited and consequently has infinite time-support. Therefore, this sampling scheme is unsuitable for finite and infinite streams of pulses. The SoS class introduced in Section II consists of compactly supported filters which is crucial to enable the extension of our results to finite and infinite streams of pulses.

Both approaches achieve the minimal number of samples. Regarding implementation, both filters cannot be implemented accurately, since analog filters are neither bandlimited nor time-limited, and therefore must be approximated. A table

comparing between the two methods is shown in Table I.

TABLE I  
PERIODIC CASE - COMPARISON WITH PREVIOUS WORK

Feature	Lowpass filter [3]	Proposed method
Degrees of freedom	$2L$	
Required no. of samples	$2L + 1$	$2L$
Time-support	Infinite	$\tau$ , finite support allows extension to finite & infinite cases
Noise Robustness	High	High
Analog implementation	Approximate lowpass filter	Approximate finite support filter. Truncated Fourier series form.

### B. Finite Pulse Stream

The authors of [3] proposed a Gaussian sampling kernel for sampling finite streams of Diracs. The Gaussian method is numerically unstable, as mentioned in [11], since the samples are multiplied by a rapidly diverging or decaying exponent. Therefore, the Gaussian approach is unsuitable for  $L \geq 6$ .

Modifications proposed in [11] exhibit better performance and stability. However, these methods require substantial oversampling, and still exhibit instability for  $L > 9$ .

The work in [12] offers compactly supported sampling kernels, which enable obtaining moments of the signal, rather than Fourier coefficients. The moments are then processed with the same annihilating filter used in previous methods. However, as mentioned by the authors, this approach is unstable for high values of  $L$ . This is due to unstable weighting of the samples when obtaining the moments, a problem that disappears when dealing with Fourier coefficients. We showed in simulations that typically for  $L \geq 5$  the estimation errors, using the B-spline sampling kernel, become very large. In contrast, our approach leads to stable reconstruction even for very high values of  $L$ , e.g.,  $L = 100$ . In addition, the moments method treats Diracs, differentiated Diracs and compactly supported filters having no DC component, whereas our approach treats any pulse with compact support.

All three methods achieve the minimal number of samples  $2L$ . A comparison is shown in Table II.

TABLE II  
FINITE CASE - COMPARISON

Feature	Gaussian filter [3]	Spline Filter [12]	Proposed method
Degrees of freedom	$2L$		
Required no. of samples	$2L$		
Time-support	Infinite	Finite	Finite
Stability	Unstable for $L \geq 6$	Unstable for $L \geq 5$	Stable even for $L = 100$
Noise Robustness	Low	Low	High

### C. Infinite Streams

Dragotti et al. [12] addressed the infinite stream case, with  $h(t) = \delta(t)$ . They proposed filtering the signal with a polynomial reproducing sampling kernel prior to sampling. If the signal has at most  $L$  diracs within any interval of duration  $LPT$ , where  $P$  denotes the support of the sampling filter and  $T$  the sampling period, then the samples are a sufficient characterization of the signal. This condition allows to divide the infinite stream into a sequence of finite case problems. In our approach the quiet phases of  $1.5\tau$  between the bursts of length  $\tau$  enable the reduction to the finite case.

Since the infinite solution is based on the finite one, our method is advantageous in terms of stability in high order problems and noise robustness. However, we do have an additional requirement of quiet phases between the bursts.

Regarding the sampling rate, the number of degrees of freedom of the signal per unit time, also known as the rate of innovation, is  $\rho = 2L/2.5\tau$ , which is the critical sampling rate. Our sampling rate is  $2L/\tau$  and therefore we oversample by a factor of 2.5. In the same scenario, the method in [12] would require a sampling rate of  $LP/2.5\tau$ , i.e., oversampling by a factor of  $P/2$ . Properties of polynomial reproducing

kernels imply that  $P \geq 2L$ , therefore for any  $L \geq 3$ , our method exhibits more efficient sampling. A table comparing the various features is shown in Table III.

Recent work [13] presented a low complexity method for reconstructing streams of pulses (both infinite and finite cases) consisting of diracs. However the basic assumption of this method is that there is at most one dirac per sampling period. This means we must have prior knowledge about a lower limit on the spacing between two consecutive deltas, in order to guarantee correct reconstruction. In some cases such a limit may not exist; even if it does it will usually force us to sample at a much higher rate than the critical one.

TABLE III  
INFINITE CASE - COMPARISON

Feature	Spline filter [12]	Proposed method
Signal model	No more than $L$ pulses in any interval of $LPT$ sec	Bursty character: burst - $\tau$ , quiet phase $1.5\tau$
Rate of innovation - bursty signal	$\rho \triangleq 2L/2.5\tau$	
Min. sampling rate	$P \cdot \rho/2$	$2.5\rho$
For $L \geq 3 \Rightarrow P/2 \geq 3$	Proposed sampling scheme is more efficient	
Noise Robustness	Low	High
Stability	Unstable for $L \geq 5$	Stable for $L = 100$

## VI. APPLICATION - ULTRASOUND IMAGING

An interesting application of our framework is ultrasound imaging. In ultrasonic imaging an acoustic pulse is transmitted into the scanned tissue. The pulse is reflected due to changes in acoustic impedance which occur, for example, at the boundaries between two different tissues. At the receiver, the echoes are recorded, where the time-of-arrival and power of the echo indicate the scatterer's location and strength, respectively. Accurate estimation of tissue boundaries and scatterer locations allows for reliable detection of certain illnesses, and is therefore of major clinical importance. The exact location of the boundaries is usually more important than the exact power of the reflection. This stream of pulses is finite since the pulse energy decays within the tissue. We now demonstrate our method on real 1-dimensional (1D) ultrasound data.

The multiple echo signal which is recorded at the receiver can be modeled as a finite stream of pulses, as in (29). The unknown time-delays correspond to the locations of the various scatterers, whereas the amplitudes correspond to their reflection coefficients. The pulse shape in this case is a Gaussian defined in (27), due the physical characteristics of the electro-acoustic transducer (mechanical damping).

In our setting, a phantom consisting of uniformly spaced pins, mimicking point scatterers, was scanned by GE Healthcare's Vivid-i portable ultrasound imaging system [19], [20], using a 3S-RS probe. We use the data recorded by a single element in the probe, which is modeled as a 1D stream of pulses. The center frequency of the probe is  $f_c = 1.7021$  MHz, The width of the transmitted Gaussian pulse in this case is

$\sigma = 3 \cdot 10^{-7}$  sec, and the depth of imaging is  $R_{\max} = 0.16$  m corresponding to a time window of<sup>2</sup>  $\tau = 2.08 \cdot 10^{-4}$  sec.

In this experiment all filtering and sampling operations are carried out digitally in simulation. The analog filter required by the sampling scheme is replaced by a lengthy Finite Impulse Response (FIR) filter. Since the sampling frequency of the element in the system is  $f_s = 20$  MHz, which is more than 5 times higher than the Nyquist rate, the recorded data represents the continuous signal reliably. Consequently, digital filtering of the high-rate sampled data vector (4160 samples) followed by proper decimation mimics the original analog sampling scheme with high accuracy. The recorded signal is depicted in Fig. 12. The band-pass ultrasonic signal is demodulated to base-band, i.e., envelope-detection is performed, before inserted into the process.

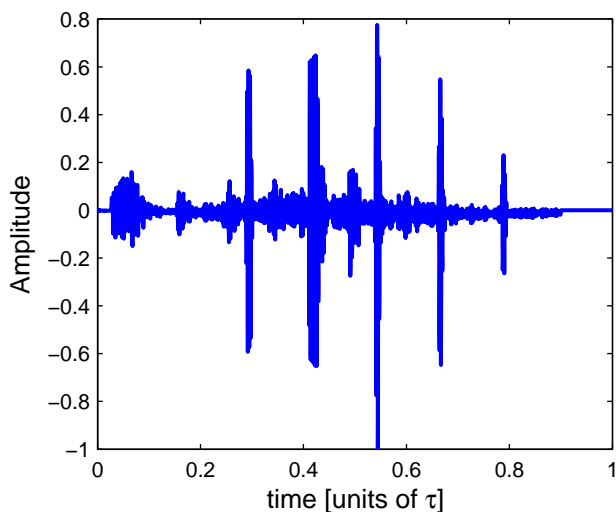


Fig. 12. Recorded ultrasound imaging signal. The data was acquired by GE healthcare's Vivid-i ultrasound imaging system.

We carried out our sampling and reconstruction scheme on the aforementioned data. We set  $L = 4$ , looking for the strongest 4 echoes. Since the data is corrupted by strong noise we over-sampled the signal, obtaining twice the minimal number of samples. In addition, hard-thresholding of the samples was implemented, where we set the threshold to 10 percent of the maximal value. We obtained  $N = 17$  samples by decimating the output of the lengthy FIR digital filter imitating  $g_{3p}^*(-t)$  from (42), where the coefficients  $\{b_k\}$  were all set to one. In Fig. 13a the reconstructed signal is depicted vs. the full demodulated signal using all 4160 samples. Clearly, the time-delays were estimated with high precision. The amplitudes were estimated as well, however the amplitude of the second pulse has a large error. This is probably due to the large values of noise present in its vicinity. However, as mentioned earlier, the exact locations of the scatterers is more important than the accurate reflection coefficients. We carried out the same experiment only now oversampling by a factor of 4, resulting in  $N = 33$  samples. Here no hard-thresholding is required. The results are depicted in Fig. 13b, and are very similar to

<sup>2</sup>The speed of sound within the tissue is 1550 m/sec.

our previous results. In both simulations, the estimation error in the location of the pulses is around 0.1 mm.

Current ultrasound imaging technology operates at the high rate sampled data, e.g.,  $f_s = 20$  MHz in our setting. Since there are usually 100 different elements in a single ultrasonic probe each sampled at a very high rate, data throughput becomes very high, and imposes high computational complexity to the system, limiting its capabilities. Therefore, there is a demand for lowering the sampling rate, which in turn will reduce the complexity of reconstruction. Exploiting the parametric point of view, our sampling scheme reduces the sampling rate by 2 orders of magnitude, from 4160 to around 30 samples in our setting, while estimating the locations of the scatterers with high accuracy.

## VII. CONCLUSIONS

We presented efficient sampling and reconstruction schemes for streams of pulses. For the case of a periodic stream of pulses, we derived a general condition on the sampling kernel which allows a single-channel uniform sampling scheme. Previous work [3] is a special case of this general result. We then proposed a class of filters, satisfying the condition, with compact support. Exploiting the compact support of the filters, we constructed a new sampling scheme for the case of a finite stream of pulses. Simulations show this method exhibits better performance than previous techniques, in terms of stability in high order problems, and noise robustness. An extension to an infinite stream of pulses was also presented. The compact support of the filter allows for local reconstruction, and thus lowers the complexity of the problem. Finally, we demonstrated the advantage of our approach in reducing the sampling rate of ultrasound imaging, by applying our techniques to real ultrasound data.

## REFERENCES

- [1] Y. C. Eldar and T. Michaeli, "Beyond bandlimited sampling," *IEEE Signal Process. Mag.*, vol. 26, no. 3, pp. 48–68, May 2009.
- [2] T. Michaeli and Y. C. Eldar, "Optimization techniques in modern sampling theory," in *Convex Optimization in Signal Processing and Communications*, Y. C. Eldar and D. Palomar, Eds. Cambridge University Press, 2010.
- [3] M. Vetterli, P. Marziliano, and T. Blu, "Sampling signals with finite rate of innovation," *IEEE Trans. Signal Process.*, vol. 50, no. 6, pp. 1417–1428, Jun 2002.
- [4] Y. M. Lu and M. N. Do, "A theory for sampling signals from a union of subspaces," *IEEE Trans. Signal Process.*, vol. 56, no. 6, pp. 2334–2345, June 2008.
- [5] Y. C. Eldar, "Compressed Sensing of Analog Signals in Shift-Invariant Spaces," *IEEE Trans. Signal Process.*, vol. 57, pp. 2986–2997, 2009.
- [6] Y. C. Eldar and M. Mishali, "Robust recovery of signals from a structured union of subspaces," *IEEE Trans. Inf. Theory*, vol. 55, no. 11, pp. 5302–5316, Nov. 2009.
- [7] K. Gedalyahu and Y. C. Eldar, "Time delay estimation from low rate samples: A union of subspaces approach," *arXiv.org 0905.2429*; to appear *IEEE Trans. Signal Process.*
- [8] M. Mishali and Y. Eldar, "Blind Multiband Signal Reconstruction: Compressed Sensing for Analog Signals," *IEEE Trans. Signal Process.*, vol. 57, no. 3, p. 993, 2009.
- [9] T. Blu, P. L. Dragotti, M. Vetterli, P. Marziliano, and L. Coulot, "Sparse sampling of signal innovations," *IEEE Signal Process. Mag.*, vol. 25, no. 2, pp. 31–40, March 2008.
- [10] P. Stoica and R. Moses, *Introduction to Spectral Analysis*. Englewood Cliffs, NJ: Prentice-Hall, 1997.

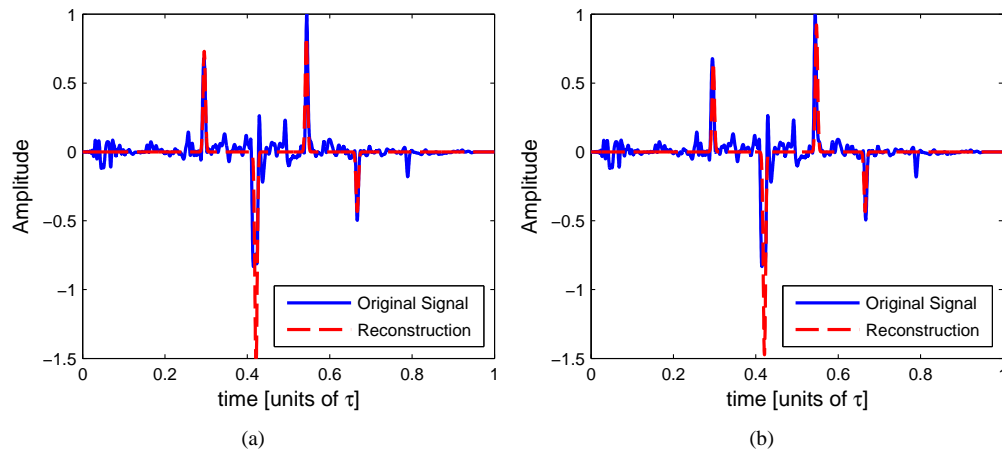


Fig. 13. Applying our  $g_{3p}(t)$  filter method on real ultrasound imaging data. Results are shown vs. full demodulated signal which uses all 4160 samples. Reconstructed signal (a) using  $N = 17$  samples only and hard-thresholding, and (b) using  $N = 33$  samples without thresholding.

- [11] I. Maravic and M. Vetterli, "Sampling and reconstruction of signals with finite rate of innovation in the presence of noise," *IEEE Trans. Signal Process.*, vol. 53, no. 8, pp. 2788–2805, Aug. 2005.
- [12] P. L. Dragotti, M. Vetterli, and T. Blu, "Sampling moments and reconstructing signals of finite rate of innovation: Shannon meets strang-fix," *IEEE Trans. Signal Process.*, vol. 55, no. 5, pp. 1741–1757, May 2007.
- [13] C. Seelamantula and M. Unser, "A generalized sampling method for finite-rate-of-innovation-signal reconstruction," *IEEE Signal Process. Lett.*, vol. 15, pp. 813–816, 2008.
- [14] B. Porat, *A course in digital signal processing*. John Wiley & Sons, 1997.
- [15] K. Hoffman and R. Kunze, "Linear Algebra, 2nd edn." 1971.
- [16] R. Schmidt, "Multiple emitter location and signal parameter estimation," *IEEE Trans. Antennas Propag.*, vol. 34, no. 3, pp. 276–280, Mar 1986.
- [17] G. Bienvenu and L. Kopp, "Adaptivity to background noise spatial coherence for high resolution passive methods," in *Acoustics, Speech, and Signal Processing, IEEE International Conference on ICASSP '80.*, vol. 5, Apr 1980, pp. 307–310.
- [18] R. Roy and T. Kailath, "ESPRIT-estimation of signal parameters via rotational invariance techniques," *IEEE Trans. Acoust., Speech, Signal Process.*, vol. 37, no. 7, pp. 984–995, Jul 1989.
- [19] R. Senior, J. Chambers, C. Roles, and N. Roles, "Portable echocardiography: a review," *British journal of cardiology*, vol. 13, no. 3, p. 185, 2006.
- [20] S. Mondillo, G. Giannotti, P. Inelli, P. Ballo, and M. Galderisi, "Hand-held echocardiography: its use and usefulness," *International journal of cardiology*, vol. 111, no. 1, pp. 1–5, 2006.